

A Short Review of Time Dependent Solutions and Space-like Singularities in String Theory

Micha Berkooz and Dori Reichmann^a *

^aDepartment of Particle Physics, The Weizmann Institute of Science, Rehovot 76100, Israel.

These lecture notes provide a short review of the status of time dependent backgrounds in String theory, and in particular those that contain space-like singularities. Despite considerable efforts, we do not have yet a full and compelling picture of such backgrounds. We review some of the various attempts to understand these singularities via generalizations of the BKL dynamics, using worldsheet methods and using non-perturbative tools such as the AdS/CFT correspondence and M(atric) theory. These lecture notes are based on talks given at Cargese 06 and the dead-sea conference 06.

1. Introduction

Over the last couple of decades string theory has provided us with a continuous stream of new ideas and insight into general relativity. Examples include the resolution of time-like singularities, either by perturbative or non-perturbative techniques, our detailed understanding of a large class of black holes, the AdS/CFT correspondence and others. Motivated by this success and by improved, observation driven, understanding of the evolution of our universe, it is very tempting to try and study time dependent solutions in String theory. This lecture will focus on a subset of such recent attempts, and in particular on backgrounds with space-like singularities and/or closed time like curves (CTC), which exist in many time-dependent backgrounds.

Despite considerable effort over the last few years, it is hard to say that we have a complete and compelling story about such backgrounds. However, some hints are beginning to emerge about the perturbative and non-perturbative effects that may play a role. This talk will be a brief review of some of these hints.

Due to the lack of space and time, the list of topics that will be covered will be partial, and many relevant and important developments will not be touched upon. The latter include the con-

struction of big-bang singularities in AdS using "designer gravity" [1,2,3,4], the "stiff equation of state" approach to big-bang singularities [5,6,7,8], String gas cosmology ([9] and references therein), pre-big-bang cosmology (for a recent review see [10]) and others. We will also not touch upon the implications to cosmology (which is one of the driving forces behind the study of time dependent backgrounds - see [11] and subsequent work). We apologize in advance for these deficiencies.

The outline of this talk is the following. In section 2 we review some of the stringy backgrounds that we will use later on. These include primarily time-dependent orbifolds. In section 3 we review the BKL dynamics, which is the generic approach to a spacelike singularity in GR. In section 4 we discuss the perturbative structure of Misner space, which is a prototype of stringy space-like singularities. In section 5 we discuss another perturbative technique, which is tachyon condensation. In section 6 we discuss non-perturbative approaches to spacelike singularities via the AdS/CFT correspondence and M(atric) theory.

2. Examples of stringy time-dependent solutions

2.1. The Schwarzschild black hole

Probably the most common example of a space-like singularity is the one in the interior of a

*micha.berkooz@weizmann.ac.il,
dor.reichmann@weizmann.ac.il

Schwarzschild black hole. The Penrose diagram of the eternal Schwarzschild black hole is given in figure 1. Regions I and I' are the two causally disconnected 'outside the horizon' regions. Each of them asymptotes to flat Minkowski space far away from the black hole. Regions II, II' are the past and future 'inside the horizon' regions (the horizons are the diagonal lines). Region II (II') ends (begins) in a spacelike future (past) singularity. The Penrose diagram, which appears in figure (1), is a convenient tool to encode the causal structure of spacetime as all particles move within (or on the boundaries) of the forward lightcone in the diagram.

The singularity inside the blackhole is closely related to the issue of time-dependence, since the solution inside the black hole is time-dependent. This is sometimes phrased as the question "what does the in-falling observer see as he/she evolves towards the singularity".

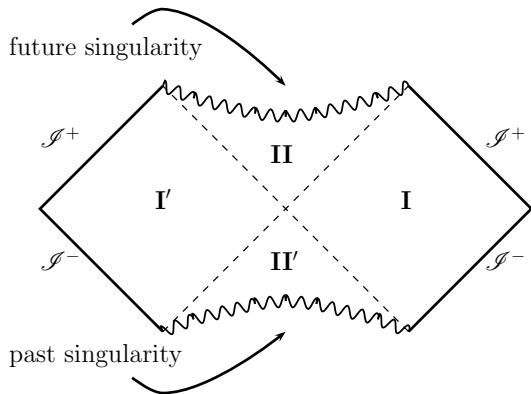


Figure 1. Penrose diagram for the Kruskal extension of the Schwarzschild black hole, showing conformal infinity as well as the two singularities.

2.2. Black holes in AdS and the BTZ black hole

The AdS analog of the Schwarzschild solution is the AdS eternal black hole. The casual structure

of the solution [14], given in the Penrose diagram in figure 2, is reminiscent of the Schwarzschild solution. The main difference is the change of the asymptotic geometry from that of flat space to that of AdS.

In AdS_3 the black hole is the BTZ black hole [12,13]. Its causal structure is actually slightly different than figure 2 - for a discussion of this issue in the context of space-like singularities see [15]. The metric of the non-rotating BTZ black hole is (setting the AdS_3 radius to 1):

$$ds^2 = -(r^2 - M)dt^2 + \frac{dr^2}{r^2 - M} + r^2 d\phi^2$$

$$\phi \cong \phi + 2\pi \quad (1)$$

Alternatively, we can use the fact that AdS_3 is the group manifold $SL(2, \mathbb{R})$ (more precisely, one may need to go to a cover of $SL(2)$ in the Minkowski case):

$$g \in SL(2, \mathbb{R}) \quad ds^2 = \text{Tr}(g^{-1}dg g^{-1}dg). \quad (2)$$

In String theory, AdS_3 with NS-NS fluxes can be promoted to a full string theory solution (for example [16] and subsequent work) by taking an $SL(2, \mathbb{R})$ -WZW model, which in addition to a non-trivial metric also includes an $H = dB \neq 0$ field on AdS_3 . The non-rotating BTZ black hole is then obtained by orbifolding the geometry by an hyperbolic element of the isometry,

$$g \cong e^{\pi\sqrt{M}\sigma^3} g e^{\pi\sqrt{M}\sigma^3} \quad \sigma^3 = \begin{pmatrix} 1 & 0 \\ 0 & -1 \end{pmatrix} \quad (3)$$

Although the BTZ space-time contains a singularity and an event horizon, the BTZ black hole geometry has constant curvature (inherited from the AdS_3 geometry), which is very low for a large AdS . The BTZ black hole might therefore be a suitable laboratory to study the singularity inside a black hole, in which we can disentangle the strong curvature effects from the effects of the spacelike singularity or CTC's.

2.3. Misner and Grant spaces

In analogy to the BTZ black hole, we wish to construct a laboratory for big-bang physics. The

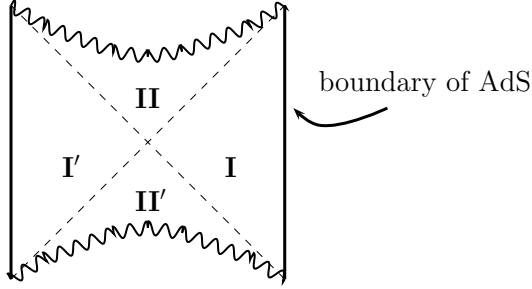


Figure 2. The AdS_d , $d > 3$, eternal black hole, the causal structure is similar to the Schwarzschild black hole only with the asymptotic boundary changed.

simplest example is Misner space, alternatively the orbifold $\mathbb{R}^{1,1} / \text{boost}$ [17,18,19]. To define the orbifold one first writes Minkowski spacetime in lightcone coordinates,

$$\begin{aligned} ds^2 &= -dt^2 + dx^2 = -dX^+ dX^- \\ X^\pm &= t \pm x \end{aligned} \quad (4)$$

and then one mods out by the Z -orbifold

$$(X^+, X^-) \rightarrow (e^{n\beta} X^+, e^{-n\beta} X^-), \quad n \in \mathbb{Z} \quad (5)$$

The action of the orbifold divides spacetime into 4 two-dimensional regions as in figure 3 (there are 4 additional one-dimensional regions on the lightcone but they will not play a role below). Regions 'future' (F) and 'past' (P), are the folding of the future and past cones (of Minkowski space) by a spacelike identification. These regions are reminiscent of a big-bang and a big-crunch regions of a cosmological model, which becomes clear if we go to coordinates:

$$\begin{aligned} T &\equiv \sqrt{X^+ X^-} & \theta &\equiv \frac{1}{2} \log \frac{X^+}{X^-} \\ ds^2 &= -dT^2 + T^2 d\theta^2 & \theta &\cong \theta + \beta \end{aligned} \quad (6)$$

Regions 'left' (L) and 'right' (R), are the folding of the left and right cones (of Minkowski space)

by a timelike identification. These regions contain closed timelike curves (CTC) since the generator of the boost is time-like there. A convenient set of coordinates is

$$\begin{aligned} R &\equiv \sqrt{|X^+ X^-|} & \eta &\equiv \frac{1}{2} \log \left| \frac{X^+}{X^-} \right| \\ ds^2 &= -R^2 d\eta^2 + dR^2 & \eta &\cong \eta + \beta \end{aligned} \quad (7)$$

We will refer to these regions as "whiskers". A

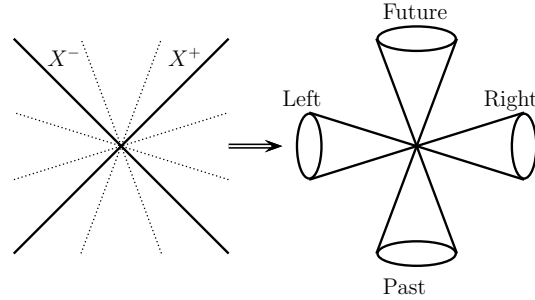


Figure 3. The Minkowski space time (on the left) is divided into 4 region by the action of the boost orbifold. The dotted lines are the boundaries of the orbifold's fundamental region, and are identified. The boost orbifold geometry (on the right) is that of 4 cones. Each quadrant of Minkowski spacetime is mapped in the orbifold to one of the orbifold's cones.

related example is the shifted boost orbifold (also known as Grant space, and discussed extensively in [20,21,22,23]). This space is defined by the addition, to the boost action, of a shift in a transverse coordinate. In terms of Minkowskian coordinates the action of the orbifold is

$$\begin{aligned} (X^+, X^-, X) &\rightarrow e^{n\hat{\zeta}}(X^+, X^-, X) = \\ &= (e^{n\beta} X^+, e^{-n\beta} X^-, X + n\Delta) \\ \hat{\zeta} &= \beta (X^+ \partial_{X^+} - X^- \partial_{X^-}) + \Delta \partial_X \\ n &\in \mathbb{Z} \end{aligned} \quad (8)$$

Due to the shift of X , the orbifold does not possess any fixed point and therefore leads to a smooth spacetime, although it still contains CTCs.

Although Grant space is smooth, one can still distinguish different regions with distinct features. There are 6 regions, which are depicted in figure 4 by projecting them to the $X^+ - X^-$ plane at $X = 0$. The 'new' region (compared to the boost orbifold) are regions B,B'. In the boost orbifold (without a shift) the Killing vector ($\hat{\zeta}$) used for the identification was spacelike in the future/past regions, timelike in the left/right region and lightlike on the lightcone. In the shifted boost case $\hat{\zeta}^2 = 0$ is a curve which lies in the left/right quadrants of Minkowski space dividing them into regions B,B' where $\hat{\zeta}$ is spacelike and regions C,C' with $\hat{\zeta}$ is timelike. Both regions B,C (and B',C') contains CTC. However, all CTCs must pass inside regions C or C', thus we can attempt to cut regions C,C' from the space-time and remove all CTCs.

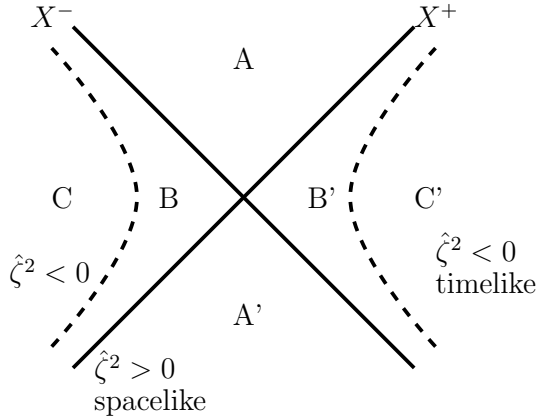


Figure 4. Minkowski space is divided by the shifted boost orbifold into 6 regions (seen at a fixed X cross section). The dashed curves is where $\hat{\zeta}^2 = 0$.

2.4. The null brane

Our last example is the null orbifold also known as the null-brane [24,25,26]. The Lorentz group in 1+2 dimensions has three classes. A Killing vector from the elliptic class (a spacelike rotation) generates the \mathbb{Z}_n orbifolds, a Killing vector from the hyperbolic class (i.e a boost) generates the boost orbifold (Misner space) and a Killing vector in the parabolic class generates the null orbifold. If one starts with a supersymmetric theory on Minkowski space, the null orbifold is the only one which will not break supersymmetry.

In terms of Minkowskian coordinates the null orbifold is defined as:

$$\begin{aligned} \begin{pmatrix} X^+ \\ X^- \\ X \end{pmatrix} &\cong e^{\nu \hat{\mathcal{J}}} \begin{pmatrix} X^+ \\ X^- \\ X \end{pmatrix} = \\ &= \begin{pmatrix} X^+ \\ X^- + \nu X + \frac{1}{2}\nu^2 X^+ \\ X + \nu X^+ \end{pmatrix} \\ \nu &= 2\pi n \quad n \in \mathbb{Z} \\ \hat{\mathcal{J}} &= X^+ \partial_X + X \partial_{X^-}. \end{aligned} \quad (9)$$

It is convenient to describe the geometry of the orbifold by introducing new coordinates

$$Y^+ = X^+ \quad Y = \frac{X}{X^+} \quad Y^- = X^- - \frac{X^2}{2X^+} \quad (10)$$

In terms of these coordinates the identification and the metric are simple

$$\begin{aligned} (Y^+, Y^-, Y) &\cong (Y^+, Y^-, Y + \nu) \\ ds^2 &= -2dY^+ dY^- + (Y^+)^2 (dY)^2 \end{aligned} \quad (11)$$

This spacetime (also called the parabolic pinch) may be visualized as two cones (parameterized by Y^+ , and Y) with a common tip at $Y^+ = 0$, times a real line (the Y^- coordinate). Y plays the role of an "angular variables" of the cones, and Y^+ plays the role of a "radial coordinate". As a function of the 'light-cone time' Y^+ we have a big crunch of the circle at $Y^+ = 0$ which is followed by a big bang. The dual role of Y^+ as both a radial variable and a time variable is the source of some interesting physics.

The down side of using the parabolic pinch coordinates is the description of the orbifold at $X^+ = 0$. In terms of the Minkowskian coordinates we identify that at the plane $X^+ = 0$ contains two co-dimension 1 cones with a common tip at $X = 0$.

2.5. Relation between the models

We have motivated the orbifolds of 3-dim Minkowski space as laboratories for cosmological models, but we can also view them as "local models" for the behavior inside the horizon of the BTZ black holes. The structure of the non-rotating BTZ black hole is given in figure 5, which contains two slices of global Minkowski AdS_3 (prior to the identification). Both slices contain the time direction and an additional spatial directions. The spatial directions of the two slices are at 90 degrees to each other. In these diagrams regions 1 and 1' are normal regions outside the horizon. Regions 2 and 2' are regions between the horizon and the singularity, and regions 3 and 3' are behind the singularity. Regions 2,2' are like P and F, and regions 3 and 3' are like L and R. They will become precisely that in the limit that the radius of curvature of AdS_3 is taken to infinity, while keep the distance to the singularity fixed. The mass of the black hole is translated to β . The addition of angular momentum to the black hole deforms the geometry such that in the large radius limit, the "near singularity" geometry is exactly that of the shifted boost orbifold, the angular momentum is translated to the shift parameter (Δ). Finally if we take a double scaling limit such that $M = J \rightarrow 0$ as we take the AdS radius to infinity we find in the near singularity are the geometry of the null brane.

There are many other models which describe string theory in time dependent backgrounds, for example [27,28,29,30,31,32] and many others. Some of the features there are similar to the ones that we will discuss here, but there are certainly many more interesting aspects in the different models. We will not have time to survey them.

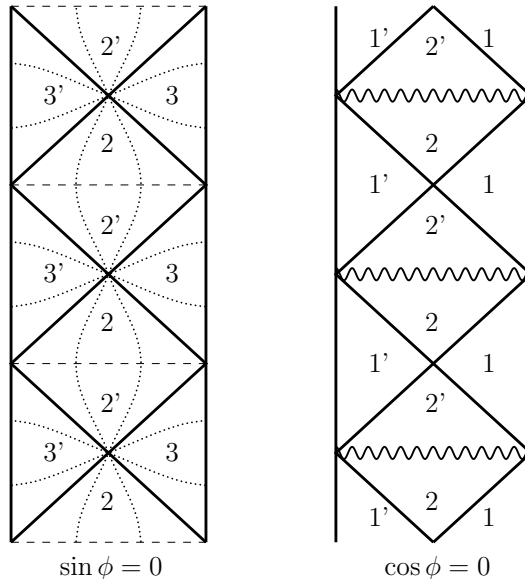


Figure 5. The geometry of the BTZ black hole (with no angular momentum) as seen from two different cross section. The cross-section on the right is the same viewpoint described earlier (figure 2) where we see the outside the horizon area (1,1') including the asymptotic boundary, the singularities and the inner horizon area's (2,2'). In the cross-section on the left we see the inner horizon areas (2,2') but also the behind the singularity areas (3,3')

3. BKL dynamics

The BKL (Belinsky-Khalatnikov-Lifshitz) [34, 33] dynamics is considered to be the generic behavior in general relativity (with potentially additional fields) near a space-like singularity. We will begin by reviewing the BKL analysis, which is a completely solvable model based on a homogeneous 3-dimensional spatial slice which collapses towards the singularity, and postpone the (less rigorous) discussion of the non-homogeneous case to later.

The starting point is the Kasner family of solutions. In this class of solutions one considers a 3

torus whose radii are allowed to vary with time, i.e.

$$ds^2 = -dt^2 + \sum_{i=1}^3 a_i^2(t) dx_i^2 \quad (12)$$

where x_i are periodic variables. A solution to Einstein's equation can be obtained by setting

$$a_i^2 \sim t^{2p_i}, \quad \Sigma p_i = \Sigma p_i^2 = 1 \quad (13)$$

(multiplication of the a_i by constants can be absorbed in the radius of x_i). Misner space, which we have discussed before, is a specific case of the Kasner solution in which $p_1 = 1$ and $p_2 = p_3 = 0$. More generally it can be shown that the solutions to the constraints (13) are such that if ordered $p_1 < p_2 < p_3$ then

$$-\frac{1}{3} \leq p_1 \leq 0 \leq p_2 \leq \frac{2}{3} \leq p_3 \leq 1 \quad (14)$$

such that generically one circle is expanding and the other two are contracting as one approached the singularity $t \rightarrow 0$.

The distinguishing feature of this class of solutions is that the spatial slice is flat. In the more generic case, some small elements of spatial curvature are turned on, rendering the approximation of a flat spatial slice inconsistent since, as the volume decreases, the curvature will increase. The details of what happens next were worked out by BKL for the case of a general homogeneous 3-dimensional space with curvature.

Since the 3 dimensional spatial slice is homogeneous, the metric can be written as

$$ds^2 = -dt^2 + dl^2 \\ dl^2 = \sum_{i=1}^3 a_i^2(t) (e_\mu^i dx^\mu) \otimes (e_\nu^i dx^\nu) \quad (15)$$

The 1-forms e_μ^i are the principal axes of the metric. The curvature of the slice is encoded in the Maurer-Cartan equations for these forms, or equivalently by

$$\lambda_i = \epsilon^{\mu_1 \mu_2 \mu_3} e_{\mu_1}^i \partial_{\mu_2} e_{\mu_3}^i / \det(e). \quad (16)$$

The classification of possible homogeneous spatial slices, or equivalently the possible λ_i , is the

Bianchi classification, which we will not review in a systematic way (a detailed exposition of this subject can be found at [35]).

Defining the new variables $a_i = e^{\alpha_i}$, Einstein's equations take on the form

$$2\alpha_{i,\tau\tau} = \left(\sum_{j \neq i} (-1)^j \lambda_j a_j^2 \right)^2 - \lambda_i^2 a_i^4, \quad (17)$$

$$\frac{1}{2} \sum_{i=1}^3 \alpha_{i,\tau\tau} = \sum_{i < j} \alpha_{i,\tau} \alpha_{j,\tau} \quad (18)$$

We will begin with a universe with low curvature, i.e., we will initially neglect the λ_i . In this case the RHS of equation (17) is zero and the solution to equation (17) is $\alpha_i = p_i \tau$. Going back to the variable t we obtain equation (13) i.e, we are back to the Kasner solutions as expected.

However, as some of the circles shrink, some elements of the curvature tensor will increase. In equation (17), one of the a_i 's is increasing, say a_1 if we choose the conventions in (14), and the RHS will be eventually non-negligible. Keeping only this term in the RHS ($a_{1,2}$ remain consistently small at this stage) then

$$\alpha_{1,\tau\tau} = -\frac{1}{2} \lambda_1^2 e^{4\alpha_1}, \\ \alpha_{i,\tau\tau} = \frac{1}{2} \lambda_i^2 e^{4\alpha_1}, \quad i = 2, 3 \quad (19)$$

which can be solved explicitly. The net result is the "BKL bounce rule". The α_1 variable, which starts with $\alpha_{1,\tau} > 0$, can be thought of bouncing off an exponential wall $\frac{1}{2} \lambda_1^2 e^{4\alpha_1}$ at large α_1 . After being reflected from the wall it will move with $\alpha_{1,\tau} < 0$ - i.e. the expanding direction turns into an contracting direction. The α_1 variable moves away from the "curvature wall" and the effects of this wall become smaller and smaller. Note that for any value of λ_1 the behavior of the wall is the same since its coefficient is λ_1^2 .

While this happens, $\alpha_{2,3}$ which initially satisfy $\alpha_{2,\tau}, \alpha_{3,\tau} < 0$ are accelerated such that these velocities are increased, but again the effects of the "curvature wall" die off as α_1 moves away from the wall. The universe now enters a new "Kasner free flight" epoch (also known as "velocity dominated epoch"). The new Kasner exponents can

be computed as described above to be

$$(p_1, p_2, p_3) \rightarrow \left(\frac{|p_1|}{1-2|p_1|}, -\frac{2|p_1| - p_2}{1-2|p_1|}, \frac{p_3 - 2|p_1|}{1-2|p_1|} \right) \quad (20)$$

Now one of the other circles is shrinking.

Another very instructive way to obtain the BKL dynamic is via a Hamiltonian formulation of GR [36]. Going to the coordinates $(\Omega, \beta_+, \beta_-)$

$$\begin{aligned} \alpha_1 &= 2(-\Omega + \beta_+ + \sqrt{3}\beta_-) \\ \alpha_2 &= 2(-\Omega + \beta_- + \sqrt{3}\beta_-) \\ \alpha_3 &= 2(-\Omega - 2\beta_+) \end{aligned} \quad (21)$$

such that Ω measures the volume of the spatial slice, the equations of motion are given by the Hamiltonian

$$2\mathcal{H} = -P_\Omega^2 + P_+^2 + P_-^2 + e^{-4\Omega}(V - 1) \quad (22)$$

together with a constraint

$$\mathcal{H} = 0. \quad (23)$$

$V(\beta)$ is determined by which elements of the spatial curvature are turned on. The Kasner case (no curvature) corresponds to $V = 1$, and the trajectory is a straight line in $(\Omega, \beta_+, \beta_-)$. In the case of Bianchi IX space $de^i = \epsilon_{ijk}e^j \wedge e^k$, which is one the cases in which all the $\lambda_i \neq 0$, we have

$$\begin{aligned} V(\beta) &= \frac{1}{3}e^{-8\beta_+} - \frac{4}{3}e^{-2\beta_+} \cosh(2\sqrt{3}\beta_-) + \\ &+ 1 + \frac{2}{3}e^{4\beta_+} \left(\cosh(4\sqrt{3}\beta_-) - 1 \right). \end{aligned} \quad (24)$$

The equipotential lines of V are drawn in figure 6. They should be thought of as receding to infinity as $\Omega \rightarrow \infty$. As the space shrinks, Ω increases and the potential goes to zero at each fixed β . The motion there is approximated by a free Kasner flight. However, if (β_+, β_-) are taken to be large enough, then we are sensitive to the potential. As $(\Omega, \beta_+, \beta_-)$ move in a straight line, they will eventually catch up with one of the walls (which are also receding as Ω increases), bounce off that wall, and move in a straight line in a different direction - this is the BKL bounce.

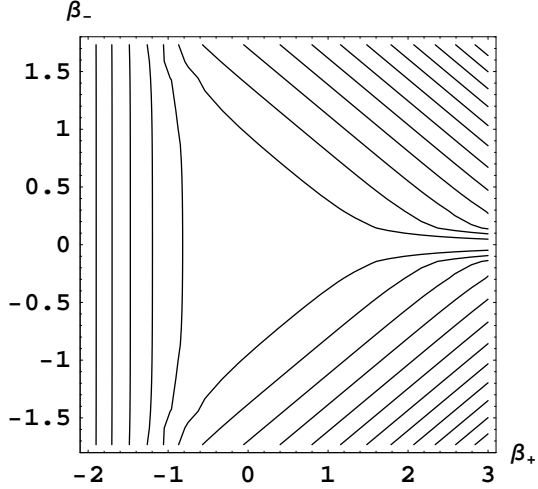


Figure 6. $V(\beta)$ for Bianchi IX spatial slice

In the regime of large (β_+, β_-) , which is relevant for small spaces or large Ω , we can truncate to the leading exponentials in $V(\beta)$. This provides us with 3 sets of walls with positive coefficients

$$V \sim \frac{1}{3}e^{-4\Omega - 8\beta_+} + \frac{2}{3}e^{-4\Omega + 4\beta_+} \cosh(2\sqrt{3}\beta_-) \quad (25)$$

The walls from which the "Kasner particle" bounces asymptote to the walls $-4\Omega + 8\beta_+ = 0$, $-4\Omega + 4\beta_+ \pm 4\sqrt{3}\beta_- = 0$. These form a pyramid in the $\Omega - \beta_+ - \beta_-$ space (which is $\mathbb{R}^{1,2}$), given in figure 7. The solution is then described by a particle moving in this wedge, such that increasing Ω corresponds to the space shrinking. The trajectory is a piecewise linear function which bounces off the walls - this has also been termed "cosmological billiards" since this system is chaotic. Note, however, that since the volume is exponential in $-\Omega$ time, the volume of space and its curvatures reach the Planck scale after only a few bounces. The analysis then breaks down since it relies on the Einstein Hilbert action.

For different extensions of GR the structure would be slightly different - if there are more fields then there would be additional degrees of free-

dom beyond $(\Omega, \beta_+, \beta_0)$, there will other walls etc. In some extensions there are not enough walls to bound the trajectory to a pyramid and it asymptotes to a straight line after a finite number of bounces. In other extensions there are enough walls and the system is chaotic. All stringy cases are of the latter type. For a review see [37].

The solution discussed so far was exact by virtue of the spatial slice being homogeneous. In the case of a generic initial condition, i.e., an arbitrary initial spatial slice one can approximate the behavior around each point by a homogeneous space. This suggests that each point moves about a pyramid of the type described above. Of course, the coefficients of the walls will change from point to point but we see that this has little effect on the dynamics. However, since the curvature at a point takes into account only the 1st and 2nd derivative of the metric around a point, one can then ask what are the effects of higher gradients. It can be argued that these contribute to sub-leading walls and hence also do not change the qualitative dynamics (again the reader is referred to [37]). This picture is supported by numerical simulations (for example [38,39]).

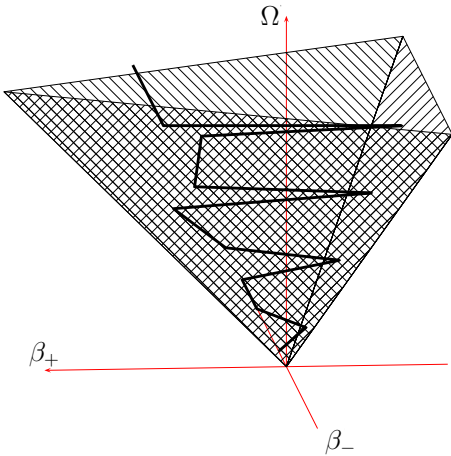


Figure 7. The BKL trajectory of a spatial slice in mini-superspace

Recently, there has been considerable renewed interest in the BKL dynamics. For a review see [37] and subsequent work of T. Damour, H. Nicolai, M. Henneaux, A. Kleinschmidt, F. Englert and others, leading to a very bold conjecture that we will mention below. The wedge that we identified above in $\mathbb{R}^{1,2}$ turns out to be the Weyl chamber of the hyperbolic algebra AE_3 with

$$A_{ij} = \begin{pmatrix} 2 & -1 & 0 \\ -1 & 2 & -2 \\ 0 & -2 & 2 \end{pmatrix} \quad (26)$$

The submatrix made out of the first two columns and rows is the Cartan Matrix of $SL(3, R)$, which arises here in the following way. If we neglect all spatial derivatives then we obtain a reduced GR action:

$$\int dt \mathcal{N}^{-1} \left(\frac{1}{4} \text{tr}((g^{-1}\dot{g})^2) - (\text{tr}(g^{-1}\dot{g}))^2 \right) \quad (27)$$

where g is the 3-metric on the spatial slice which is $SL(3)$ and N is the lapse function. The appearance of AE_3 is more mysterious, but it turns out that for all dimensions and extensions of general relativity, in which the BKL system is chaotic, such an algebra can be identified such that the BKL motion is given by a Weyl chamber. For M-theory the algebra is E_{11} . This has led these authors to conjecture that M-theory can be formulated via a sigma model on this algebra.

4. Perturbative approaches to spacelike singularities

4.1. Quantization of Misner space

The geometry of Misner space is described in figure 3. Region P (F) describes a big crunch (big bang) and regions L and R (called "whiskers") are regions with CTC's - these regions are Rindler spaces with compact Rindler time. Convenient coordinates for the different regions are given in (6) and (7).

This model is, in fact, taken to be a "local model" for the emergence of CTC's in Hawking's chronology protection conjecture paper [40]. Taking region P with metric $ds^2 = -dt^2 + t^2 dx^2$, one can carry out a change of coordinates $\tau = t^2$, $v = \ln(t) + x$ to bring the metric to the form

$ds^2 = -dv d\tau + \tau dv^2$ which covers region P for $\tau > 0$ and region R for $\tau < 0$. The symmetries of the space then determine that a conformally invariant field on this space, times R^2 , will have an energy momentum tensor

$$\langle T \rangle \propto \text{diag}(t^{-4}, 3t^{-4}, -t^{-4}, -t^{-4}). \quad (28)$$

This is one of the motivations for the conjecture that the divergence of the energy-momentum tensor on the boundary of the region where CTC's appear will prevent them from forming.

In this section we will discuss the quantization of String theory in this background as an orbifold, which turns out to be subtle. We will begin with the simplest sector, which is the untwisted sector, which already exhibits some unusual features.

The untwisted sector

The untwisted sector states are obtained by symmetrizing flat space wave functions with respect to the Z action of the orbifold [18], i.e.,

$$f_{j,m^2,s}(x^+, x^-, x) = \int_{-\infty}^{\infty} dv \cdot \exp\left(ip^+ X^- e^{2\pi\beta v} + ip^- X^+ e^{-2\pi\beta v} + ivj + vs\right) \quad (29)$$

where m is the mass of the particle, s is its spin and j is the boost angular momentum (which is discrete). We will focus on the case $s = 0$ (for a discussion of the precise definition of this wave function in the case $s \neq 0$ see [41]).

Note that since the orbifold action does not reverse the orientation of time, the Misner orbifold maintains the division between positive and negative energies inherited from flat space. Hence there is no particle creation in this background. This is similar to the null brane model [24,25].

Correlation functions for scalars in the untwisted sector states were calculated in [42]. 2 and 3-pt functions are well behaved but the 4-pt functions diverges as in [24,25] for the null brane. Since each vertex operator in the untwisted sector is an integral over the flat space vertex operator, we simply integrate the 4-pt function with 4 integrals of the type (29). Out of these 4 v_i variables, two are fixed by momentum conservation in terms

of the other two, and one factors out since it is an overall boost of the entire system, which gives the volume of the angle of the orbifold. One is left with a single non-trivial integration. If $\Psi_{1,2}$ are the incoming wave functions and $\Psi_{3,4}^*$ the outgoing ones then the stringy S-matrix (i.e., the integrated 4-pt function) is

$$\begin{aligned} & \langle \Psi_1 \Psi_2 \Psi_3^* \Psi_4^* \rangle = \\ & \int_0^\infty G(s(v_4)) G(t(v_4)) G(u(v_4)) \cdot \\ & \cdot v_2^{il_2+1} v_3^{-il_3+1} v_4^{-il_4-1} \left| m_2 m_3 (v_2^2 - v_3^2) \right| \end{aligned} \quad (30)$$

where $v_{2,3}$ are functions of v_4 (we will not need the details of these functions), s, t, u are the Mandelstam variables of the $2 \rightarrow 2$ process that we are discussing, and $G(x) = \Gamma(-1 - x/4)/\Gamma(2 + x/4)$.

In the limit $v_4 \rightarrow \infty$, $v_2 \propto v_4$ and v_3 is constant. We are interested in this limit in order to see whether the integral diverges. In this limit, one also obtains the relations $t \rightarrow -(\vec{p}_1 - \vec{p}_3)^2$ and $s = m_1 m_2 v_4$. The integral then becomes (up to a numerical coefficient)

$$\begin{aligned} & \propto (m_1 m_4)^{1-\frac{1}{2}(\vec{p}_1 - \vec{p}_3)^2} \left(\frac{m_4}{m_2}\right)^{il_2} \left(\frac{m_3}{m_1}\right)^{-il_3} \\ & \cdot \frac{\Gamma(-1 + \frac{1}{2}(\vec{p}_1 - \vec{p}_2)^2)}{\Gamma(2 + t/4)} \cdot \int_0^\infty dv_4 v_4^{t/2+i(l_2-l_4)} \end{aligned} \quad (31)$$

which is divergent for $|t| < 2$. Qualitatively, it is a UV divergence that occurs only when distances in the transverse direction are large enough, and hence has been given the name "IR enhanced UV divergences" [24,25].

So string theory does not fully remove the divergences. The divergence is still milder than in GR though. In the limit $\alpha' \rightarrow 0$, the dependence on t in the integrand vanishes (since it is really v_4 to the power $\alpha' t + \dots$), and the integral diverges for all values of t . In the limit $\alpha' \rightarrow 0$ it is also easy to identify that the origin of the divergence is due to a pole in the t-channel exchange of a

graviton

$$\int d^8x \int dx^+ dx^- \partial_- \Psi_1 \partial_- \Psi_3^* \frac{1}{\partial^2} \partial_+ \Psi_2 \partial_+ \Psi_4^* \quad (32)$$

The effect of a UV divergence associated with larger transverse separation can be expected on the following grounds [43]. Consider two particles on the orbifold and evaluate their interaction by going to the covering space $\mathbb{R}^{1,1}$, keeping a single image of one of them and considering its interactions with all the images of the other, which are related by the boost $\exp(n\beta J_{+-})$ for all integer n . The relative boost between particle 1 and the images of particle 2 therefore increases (indefinitely). Since their center of mass energy is increasing and the impact parameter does not, then when the latter is below the Schwarzschild radius of a black hole with the same mass, the process will be dominated by black hole formation. The size of black hole in the transverse also grows larger and larger with n , hence we expect a correlation between the UV divergences in the theory and large distances in the transverse direction.

Twisted sector

We will begin by discussing a seemingly unrelated system - that of a charged open string in an electric field [44] (which is T-dual to a pair of branes at relative velocity [45]). This system can be realized by taking a pair of D-branes and turning on an electric field on one of them, or by turning on an opposite electric field on the two branes. Open strings in an electric field are given by the boundary conditions

$$\begin{aligned} \partial_\sigma X^\pm &= \mp \pi e \partial_\tau X^\pm & \sigma = 0 \\ \partial_\sigma X^\pm &= \pm \pi e \partial_\tau X^\pm & \sigma = \pi \end{aligned} \quad (33)$$

The mode expansion is therefore

$$\begin{aligned} X^\pm &= x_0^\pm + i \sum_{n=-\infty}^{\infty} (-1)^n \frac{\alpha_n^\pm}{n \pm i\nu} e^{-i(n \pm \nu)\tau} \\ &\quad \cos[(n \pm i\nu)\sigma \mp i \cdot \text{arcth}(\pi e)] \end{aligned} \quad (34)$$

and the commutation relations are

$$\begin{aligned} [a_m^+, a_n^-] &= -(m + i\nu) \delta_{m+n}, \\ [x_0^i, x_0^j] &= -i/2e \end{aligned} \quad (35)$$

Next we need to choose a realization of this algebra, i.e, determine the Hilbert space and the ground state. The choice for the excited states $n \neq 0$ is straightforward, since the energy of the state has a real part by which we can divide the operators into creation and annihilation. The choice for a_0 is slightly more complicated. However, in the limit $e \rightarrow 0$, the a_0^\pm are simply the momenta of the particle. Hence one realizes these operators as [19] simply as the momentum in the presence of an electric field

$$\begin{aligned} a_0^\pm &= p^\pm = i\partial_\mp \pm \frac{\nu}{2} x^\pm, \\ x_0^\pm &\propto i\partial_\mp \mp \frac{\nu}{2} x^\pm \end{aligned} \quad (36)$$

and the coordinates x_0^\pm are the coordinates of the center of the hyperbola on which a charged particle moves in an electric field.

The Hilbert space is then simply $L^2(\mathbb{R}^{1,1})$. With this realization the correct normal ordering prescription for the worldsheet energy-momentum tensor is

$$\begin{aligned} L_0 &= -\frac{1}{2}(a_0^+ a_0^- + a_0^- a_0^+) + \frac{1}{12}(\nu^2 - 1) + \\ &\quad + \text{excited states} \end{aligned} \quad (37)$$

which is the just the charged particle Klein-Gordon equation.

Going back to closed strings on Misner space [19], the twisted boundary conditions are

$$X^\pm(\sigma + 2\pi, \tau) = e^{\pm w\beta} X^\pm(\sigma, \tau), \quad w \in Z \quad (38)$$

give rise to mode expansion

$$\begin{aligned} X_R^\pm(\tau - \sigma) &= \frac{i}{2} \sum_{n=-\infty}^{\infty} \frac{\alpha_n^\pm}{n \pm i\nu} e^{-i(n \pm i\nu)(\tau - \sigma)} \\ X_L^\pm(\tau + \sigma) &= \frac{i}{2} \sum_{n=-\infty}^{\infty} \frac{\tilde{\alpha}_n^\pm}{n \mp i\nu} e^{-i(n \mp i\nu)(\tau + \sigma)} \\ [\alpha_m^+, \alpha_n^-] &= -(m + i\nu), \\ [\tilde{\alpha}_m^+, \tilde{\alpha}_n^-] &= -(m - i\nu) \end{aligned} \quad (39)$$

where $\nu = w \cdot \beta$. Following the example of the open string in electric field we will choose

the Hilbert space to be $L^2(\mathbb{R}^{1,1})$ and the realization of the operators is the same as in (36) with $a_0^\pm \rightarrow \alpha_0^\pm$ and $x^0 \rightarrow \tilde{\alpha}_0$ (and the \propto sign replaced by an equality). Both the left and right energy-momentum tensor is similar to (37) with $L_0 - \tilde{L}_0 = 2\nu j$ where j is the quantum number under boosts which is quantized to be an integer. From now on we will focus on the pseudo zero-modes and neglect the oscillators (they will play an important role in a computation below though).

Focusing on the zero modes, the oscillators and mass-shell conditions translate into equations on the quasi-zero modes of the form

$$M^2 = 2\alpha_0^+ \alpha_0^-, \quad \tilde{M}^2 = 2\tilde{\alpha}^+ \tilde{\alpha}_0^- \quad (40)$$

For simplicity we will focus on the case $M^2 - \tilde{M}^2 = 0$ (recall that the difference between them is the boost momentum). By shifting in τ and boosting (shifting in σ) we can reach a situation where the modulus of $\alpha_0^\pm, \tilde{\alpha}_0^\pm$ are all equal. In this case, semiclassically, these equation have two distinct branches of solutions

1) "short strings": $sign(\alpha_0^+) = sign(\tilde{\alpha}_0^+)$ where the classical string takes the shape

$$X^\pm(\tau, \sigma) = \epsilon \frac{M}{\nu\sqrt{2}} \sinh(\tau) e^{\pm\nu\tau}. \quad (41)$$

This is a string that is moving from region P into region F (F into P) for $\epsilon = 1$ ($\epsilon = -1$).

2) "long strings" $sign(\alpha_0^+) \neq sign(\tilde{\alpha}_0^+)$, in which case the profile is

$$X^\pm(\tau, \sigma) = \pm\epsilon \frac{M}{\nu\sqrt{2}} \cosh(\tau) e^{\pm\nu\tau}. \quad (42)$$

For $\epsilon = +1$ (-1) this is a string which wraps the time direction in whisker R (L), and in the radial direction comes in from infinity to some finite distance from the origin and then goes out to infinity again.

Next we would like to ask whether these strings, and primarily the "long strings", do anything interesting. One can either condense them or ask whether they are created in pairs - if one starts from a configuration in which the twist quantum number is conserved then only the latter is allowed. Next, one can try and evaluate how such

strings backreact on the geometry, an issue which is not well understood (see however [47]). Here we will briefly go over one of the arguments that these strings are pair produced, after carefully considering the 2nd quantization (in space-time) of the model [41].

We have seen that there are two types of strings - "short" and "long". The short strings have a unique vacuum - strings propagating forward in time are creation operators and those backwards in time are annihilation operators. For the long strings the ground state is ambiguous. This can be understood as follows: the closed strings quasi-zero-modes can be viewed as two copies of the momentum of a charged particle in an electric fields, or we can take the left moving quasi-zero-modes to be momenta and the right movers to be the center the hyperbola, or we can switch the role of the left and right movers. Each choice like this has a different natural vacuum. In all these vacua there is either twisted sector particle pair creation, just as particles in an electric field, or a large degeneracy of vacua which one needs to sum over.

3-pt function:

One way of possibly evaluating the effects of condensation of twisted modes on the geometry is to try and use conformal perturbation theory. Although we may not expect that this will make the model completely non-singular, it might give us some information. The first step is to evaluate a 3-pt function of 2 twisted sector states and one untwisted. This will also give us information on how the regular graviton sees the twisted sector states, ie., what is their profile of $\langle T_{\mu\nu} \rangle$. This was carried out in [46].

The simplest way to carry out the computation of a 3-pt function with two twisted sector vertex operators and a single untwisted vertex operator is to insert the twisted operators at $\tau \pm \infty$ on a cylinder, and the untwisted vertex operator somewhere in between, which means computing a 1-pt function of an untwisted operator in the twisted sector. We will focus on a universal stringy part of the result, which is due to the excited string modes. The latter turns out to be reminiscent of non-commutative geometry.

The untwisted vertex operator is defined in the

untwisted sector as

$$V_T = \lim_{w \rightarrow z} e^{ik^+ X^-(w)} e^{ik^- X^+(z)} e^{k^+ k^- \log(w-z)} \quad (43)$$

When we insert this operator in the twisted sector, the simplest way to carry out the computation is to re-normal-order it with respect to the twisted sector vacuum:

$$\begin{aligned} V_T &= e^{i(k^+ X_{<0}^- + k^- X_{<0}^+)} e^{i(k^+ X_{>0}^- + k^- X_{>0}^+)} \\ &e^{i(k^+ X_0^- + k^- X_0^+)} e^{k^+ k^- ([X_{>0}^-, X_{<0}^+] - [X_{>0}^-, X_{<0}^+])} \end{aligned} \quad (44)$$

where $X_{<}$ ($X_{>}$) is the creation (annihilation) part of X with respect to the twisted vacuum, and $X_{>}$ and $X_{<}$ the similar parts with respect to the untwisted vacuum.

The last exponential is simply

$$e^{-k^+ k^- (\psi(1+i\nu) + \psi(1-i\nu) - 2\psi(1))}. \quad (45)$$

At large values of $\nu \sim \beta w$, where w is the twisted sector number, the coefficient of $k^+ k^-$ is $-2 \cdot \ln(\nu)$, i.e., arbitrarily large. For any wave function that we take for a twisted sector state $\Psi(x^+, x^-)$, ordinary untwisted string states will see them smeared (by an amount which can be very large) by the kernel (45) acting on $|\Psi|^2$. This non-locality is similar to the one seen in non-commutative geometry - wave functions which have higher k^+ momentum will be more delocalized in the k^- direction.

5. Tachyon condensation

we have focused before on twisted sector modes in the general Misner orbifold. Let us now specialize to the case that the rate in which the orbifold decreases is small, i.e, $\beta \ll 1$, or conversely $\dot{R} \ll 1$ in region P where we have a circle of radius R shrinking to zero [49].

In this case, when the radius of shrinking circle reaches about the String scale, and if the fermions have anti-periodic boundary conditions around the orbifold (a Scherk-Schwarz compactification [48]), the lowest winding state becomes tachyonic. Since we have assumed that $\dot{R} = \beta \ll 1$ at $R \sim l_s$, the singularity is still a long time ahead

in the future, l_s/β , and we can deal with the effects of the condensation of this tachyon without worrying about the singularity [49] (more complicated collapsing geometries are discussed in [50] and application to the "final state of the black hole" [51] are discussed in [52]).

The condensation of a tachyon in a time direction is not understood as much as the condensation of tachyon on a time-like singularity, i.e., a tachyon localized along a spatial direction. Nevertheless, we will use the latter to get some intuition. Furthermore, tachyon condensation in closed strings is not as well understood as in open strings (for a review see for example [53]), but the general features will suffice for our purposes.

In [54] it was shown that non-supersymmetric orbifold singularities relax to flat space (or to supersymmetric orbifold singularities) by condensing twisted sector closed string tachyons. Geometrically, the orbifold looks like a cone, whose tip is resolved by String theory. In the case that the singularity relaxes to flat space, the condensation of the tachyon removes the tip of the cone and smoothes it out (when the tip of the cone has been smoothed to below string scale curvatures one can use GR to describe its relaxation to flat space). We see that the condensation of a localized tachyon excises the part of space where the tachyon profile is localized. This can be understood generally from worldsheet considerations - the condensation of the a tachyon decreases the central charge on the worldsheet (remember that we are discussing the static spatial part of the target space, which is unitary) and therefore removes degrees of freedom. In particular it can remove the degrees of freedom that correspond to string states moving in that region of space - hence parts of space are removed. Another class of localized tachyons is discussed in [63].

A similar process can be exhibited in the context of the AdS/CFT duality. The Hawking-Page phase transition is understood to be a confinement/de-confinement phase transition in the dual field theory [56]. In [57] it was shown that this phase transition can be understood as a condensation of a localized Atick-Witten tachyon, which is easy to identify if thermal AdS is superheated (tachyons play additional important

roles in AdS - for example see [55,62] and references therein). Another clean model in the context of closed strings is the FZZ duality between $SL(2)/U(1)$ (the Euclidean two dimensional black hole) and sine-Liouville theory [58] (more information on this duality can be found at [59] and subsequent work. The supersymmetric case is discussed in [61,60]). The $SL(2)/U(1)$ background is

$$\begin{aligned} ds^2 &= k(dr^2 + \tanh^2 r d\theta^2), \quad \theta \sim \theta + 2\pi \\ \Phi &= \Phi_0 - 2 \ln(\cosh(r)) \end{aligned} \quad (46)$$

i.e, it is a space which starts as an $S^1 \times$ (linear dilaton) at infinity and caps off by pinching the S^1 at some finite value of the dilaton. The sine-Liouville background is given by the 2D lagrangian

$$\begin{aligned} L &= \frac{1}{4\pi} \left((\partial x)^2 + (\partial \phi)^2 + Q \hat{R} \phi + \right. \\ &\quad \left. + \lambda e^{-Q/b} \cos[R(X_L - X_R)] \right). \end{aligned} \quad (47)$$

In this case there is no geometric end at the strong coupling region, but rather there is a winding mode, similar to the tachyon we have discussed above, whose profile increases in the strong coupling region. Since the two models are the same quantum mechanically, we see that the main effect of this winding mode condensate is to excise the region of space where it condenses.

In the context of a time dependent background and a state becoming tachyonic at a given moment in time and onwards, we expect that the condensation of this tachyon will cut the time direction [49]. In the case that we are discussing, since $\beta \ll 1$, this happens long before one reaches the singularity and hence one needs not worry about it or about the large blue shift effects associated with it. The hope is that this new kind of cap will have finite stringy amplitudes.

There are two approaches that one can take. In both of them one starts with an ordinary spacelike Liouville theory

$$S = \int \frac{d^2 \sigma}{4\pi} \left((\partial \phi)^2 + \mu e^{2b\phi} \right) \quad (48)$$

with a background charge $Q = b + 1/b$. One can then either use the Euclidean solution, whose correlation functions are finite and well understood, as a kind of Hartle-Hawking state [64], which is the approach taken in [49,67,50,68], Or one can try and solve it in Minkowski space [65,66,52].

Both approaches have some intriguing features, but are not without open problems. The idea that the condensing tachyon is a uniquely stringy Hartle-Hawking cap is very appealing. But since the problem is inherently Minkowskian it relies on the assumption that the analytic continuation is well defined, whereas it is clear that it is very subtle. Also, using a Hartle-Hawking state requires that one will be able to glue the Euclidean cap to a Minkowskian spacetime such that we will inherit a Minkowskian initial condition. It is not clear how to do so for Liouville theory which does not have a $\phi \rightarrow -\phi$ symmetric slice.

Studying the Minkowskian setup directly also produces some unusual features. If one attempts to define it via the analytic continuation of the Euclidean Liouville with $\phi = iX^0$ and β purely imaginary then one can show that it does not satisfy all axioms of CFT [65] (certain 3-pt functions do not reduce to 2-pt functions upon insertion of the identity operator as one of the 3 operators). A direct quantization of the model in Minkowski space has been carried only in mini-superspace thus far [66]. The Minkowskian model

$$\mathcal{L} = (\partial_\tau X^0)^2 + \mu e^{\beta X^0}, \quad \mu > 0 \quad (49)$$

describes a particle moving in an inverted exponential potential. Such a particle reaches $X^0 = \infty$ at finite time. Hence one needs to supplement boundary conditions at infinity (or more radically one can attempt to glue it to another space altogether). Already in minisuperspace these boundary conditions are not unique, but rather parameterized by a single real number, and it remains to be seen what happens in the case of a full field theoretic analysis.

For further reading on recent progress in the understanding of time-like and null tachyons the reader is referred to [69,70,71,72].

6. Non-perturbative methods

6.1. Using the AdS/CFT

As we discussed in section 2, inside the Schwarzschild black hole there exists a space-like singularity. In this section we will describe some of the efforts to understand such singularities in the context of black holes in AdS, using the AdS/CFT correspondence.

6.1.1. Simulation of black holes, microstates, and the state at the BH singularity

The statement of the AdS/CFT correspondence [73] is that a field theory, which is an object that we understand rather well quantum mechanically, is completely equivalent (or more precisely dual via a strong/weak coupling duality) to a gravitational background. A thermal state in the field theory is dual to a non-extremal black hole on the gravitational side. The most straightforward way therefore to probe a black hole is simply to run a simulation of the thermal state in the field theory.

In practice, a full simulation is not doable since we need to take the large N limit to obtain a weakly curved gravitational background. However a mean field simulation of the field theory for D0-branes (i.e, quantum mechanics) was carried out in [74,75,76,77] with reasonable agreement to the black hole behavior in the gravity dual to D0-branes [78].

One can then ask whether one sees any remnant of the singularity. The answer is that it is difficult to see any remnant of the region behind the horizon at all. The black hole is described by a thermal state, and probe computations, with which spacetime is defined in this framework, breakdown at the horizon - a D0 brane probe which is brought close to the cluster of thermalized D0 branes will simply thermalize once it reaches the vicinity of the horizon. This thermalization is signaled by the appearance of a tachyon in the off-diagonal mode between the probe D0 brane and one of the D0 branes in the thermal state.

In this picture the whole region behind the horizon is replaced by the thermal state. This pic-

ture is reminiscent of the micro-state or fuzzball picture of the black hole advocated by Mathur (for a review see [83]). In this picture the black hole is replaced by an ensemble of classical GR solution without horizons. These solutions are very similar in the region outside the would-be horizon but are very different inside it where they develop a multi-throat cap. In this description the singularity also disappears (and in fact spacetime is regular, singularity free and horizon free throughout the solution). The black hole is considered to be, in such a picture, an effective description of the ensemble of such states. The caveat is that actually the different configurations differ only on very small scales, which means that under any small perturbation they will start mixing extensively, which might indicate that the ensemble picture is always the correct description. Still it could be that for the study of the singularity one needs to go back to the micro-state language - to our knowledge this has not been done.

A related development is the suggestion by Horowitz and Maldacena [51] that for the purposes of computing in the low energy effective action, one needs to place a specific state at the spacelike singularity. This might make the evolution from past null infinity to future null infinity unitary in the region outside the black hole. To make contact with the discussion before, since the singularity is in the future of all observers behind the horizon, one can take the state at the singularity and evolve it backwards in time to a state at the horizon, i.e., we end up with a description in which we have cut space at the horizon and replaced it by some new complicated state. Actually, if the thermal state description in the D0 quantum mechanics could be clarified, or how to sum over the GR microstates, this could be a way to calculate the state at the black hole singularity.

6.1.2. The eternal black hole in AdS spaces

The Penrose diagram of the eternal black hole in AdS_d ($d > 3$) is given in figure 2 [14] (the case $d=3$ is special and is described in [15]). This configuration is dual to the thermofield description of finite temperature field theory [79]. The state in the field theory which is dual to the black hole

is the thermal density matrix

$$\rho = \sum_n e^{-\beta E_n} |n\rangle \langle n| \quad (50)$$

where the sum over n is a sum over energy eigenstates which span the physical Hilbert space \mathcal{H} . Note, however, that the eternal Minkowski black hole has two boundaries which are $S^3 \times R$. This geometry is encoded by going to the thermofield description, which is a different way of writing the density matrix above. In this description one uses a pure state in a doubled Hilbert space $\mathcal{H} \otimes \mathcal{H}$ (with hamiltonian $H = H_1 - H_2$)

$$|\Psi\rangle = \sum_n e^{-\beta E_n/2} |n\rangle_1 * |n\rangle_2 \in \mathcal{H} * \mathcal{H} \quad (51)$$

up to a normalization. A correlation function of operators $O(t_i)$, which act on the first copy of \mathcal{H} , in this state satisfies

$$\langle \Psi | O(t_1) \dots O(t_n) | \Psi \rangle = \text{tr} \left(\rho \cdot O(t_1) \dots O(t_n) \right) \quad (52)$$

(at different times and positions, when we are suppressing the latter).

In the thermofield description, however, we now have the option to act with operators on either Hilbert spaces. Let us take two operators $A(t_1)$ and $B(t_2)$ and denote on which Hilbert space they act by using an additional lower index 1 or 2. An operator $O_1(t)$ ($O_2(t)$) acts on the first (second) copy of \mathcal{H} . In this case, the following relation holds

$$\begin{aligned} \langle \Psi | A_1(t_1) B_2(t_2) | \Psi \rangle &= \\ &= \langle \Psi | A_1(t_1) B_1(t_1 - i\beta/2) | \Psi \rangle. \end{aligned} \quad (53)$$

Hence there is an easy interpretation for computing correlators with insertions on both boundaries of the eternal BH.

The question is whether we can compute some correlators on the boundary that will probe the singularity. We will then try and evaluate these correlators in the dual field theory, and see how the singularity changes as g_s is taken to be non-zero (finite N), or when string worldsheet corrections are taken into account (smaller 't Hooft coupling).

Whether we can find such correlators is not a priori clear. On the one hand the Minkowskian black hole is the analytic continuation of the Euclidean black hole. In the latter, the background terminates at the horizon, well before reaching the singularity. This background in itself contains most of the physical information about the thermal field theory, leading one to expect that we will not be able to observe anything behind the horizon. On the other hand, if one inserts two operators on the two boundaries then the propagator probes the region behind the horizon and one can attempt to probe the singularity this way [14,15].

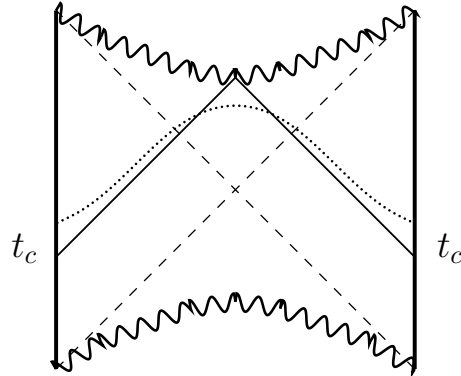


Figure 8. The dotted line is a geodesic going from one boundary to the other. The solid line is the critical null geodesic which touches the singularity.

Focusing on very massive particles, the propagator is dominated by a single space-like geodesic which goes through the horizon. For AdS_d $d > 3$ one can choose points on the two boundaries such that the geodesic between them passes as close as we want to the singularity, and its proper length in the interior is as small as we want (i.e., it approaches a null geodesic). In fact there are two critical points, each one at time t_c on each of the boundaries, such that the geodesic between these

points is null and touches the singularity (figure 8). The existence of such a geodesic implies that $\langle \Phi(t_c)\Phi(t_c - i\beta/2) \rangle$ diverges. So it seems that there is a signature for the singularity [14].

This raises a puzzle. The fact that the two point function diverges is actually in contradiction to an inequality in finite temperature field theory

$$|\langle \Phi_1(t)\Phi_2(-t) \rangle| < \langle \Phi_1(0)\Phi_2(0) \rangle < \infty \quad (54)$$

This inequality indicates that in the Minkowskian black hole, viewed as an analytic continuation of the Euclidean black hole, one is not supposed to take this geodesic into account. This is a situation which is known to happen when evaluating integrals (in this case, a path integral) via the steepest descent method - the largest saddle point need not dominate if it is not on a good steepest descent contour. Hence, it seems that again we do not see the singularity.

However, this geodesic, i.e saddle point in the Green's function, is still there. We can analytically continue time in this Green's function even further then the $\pi/2$ rotation that takes us from Euclidean to Minkowski space such that in this new non-physical regime, the null geodesic will be the dominant contribution. Hence, there will be a pole in the correlation function in some non-physical sheet. In principle one can try and see if such a pole exists and study its behavior as N and the 't Hooft coupling are varied. In [80] preliminary results were presented that the pole does not exist at large N , weak 't Hooft coupling (using an approximation of the correlator which is then analytically continues to the non-physical sheet). This may indicate that the singularity is smoothed out already by α' effects. However, this assumes that the procedure of extracting the pole is reliable, which is not a settled issue yet. A detailed description of the analytic structure of the finite temperature field theory, some more observables that one can construct and a discussion of what it might take to measure them with enough precision is given in [81,82].

6.2. M(atr)ix models

A BFSS [84] type Matrix model for a linear dilaton background in a null direction, $g_s =$

e^{-Qx^+} , was discussed in [89] and [87]. Transforming to the Einstein frame this gives us a big-bang configuration. The M(atr)ix model turns out to be 1+1 SYM with a varying Yang-Mills coupling in the field theory. Since the string coupling becomes strong (weak) at the early (late) times, the YM coupling is weak (strong) there [85]. Equivalently by a scale transformation, one can describe the model as a 1+1 SYM with fixed coupling on a worldsheet which looks like the future cone of Misner space. A M(atr)ix model for the null brane was discussed in [88] and [86], and it also turns out to be a time-dependent lagrangian on the worldvolume of the matrix theory. A D-Instanton probe of the null-brane singularity was done in [47].

These models share several features, so we will discuss them together. We will begin with some caveats and then focus on the physics that can be extracted from the models. The first caveat is that both models rely on a perturbative analysis of the closed string background, and do not allow for changing the background in a large way. This is worrisome since we believe that these backgrounds are unstable as they have large divergences. Another issue, which was addressed in the papers, is that the theory on the D0 or D1 branes breaks supersymmetry. In such cases very often a non-supersymmetric brane configuration generates tadpoles for closed string modes and one needs to condense these modes, go to the stable point, and only then decouple the theory on the open branes. Furthermore, without SUSY there is no guarantee that the perturbative computation will give the same results as the large N , very low energy, $(1/N)$, computation required for the BFSS conjecture.

Our approach will be the following. First of all, even without using a BFSS like conjecture, these models provide information on the behavior of stringy probes near the singularity. Second, if relying on a BFSS like conjecture, we will view the results of the M(atr)ix analysis as indicating some general features of the behavior near the singularity, rather than a full qualitative computational tool.

The result that is obtained in both models is that near the singularity, the full $N * N$ degrees of

freedom of the matrices need to be used. Usually when the full $N * N$ degrees of freedom are excited (and assumed in a thermal phase) one obtains the M(atrix) description of a black hole [91,90]. For the null brane this has a clear interpretation in the spirit of the Polchinski-Horowitz effect - as the D0 branes (or gravitons in a BFSS interpretation) are squeezed together near the singularity, they form black holes and the full set of degrees of freedom of the black holes have to be used. In the case of the linear dilaton background, the interpretation is less clear but seems to indicate a new non-geometrical phase at the big bang singularity (perhaps reminiscent of the "gas of black holes" or "maximally stiff equation of state" hypothesis of [5,6,7,8]).

7. Acknowledgement

It was a pleasure talking with many people on these subject - O. Aharony, B. Craps, B. Durin, S. Elitzur, F. Englert, A. Giveon, Z. Komargodsky, D.Kutasov, H. Liu, B. Pioline, G. Rajesh, E. Rabinovici, V. Schomerus, S. Sethi, S. Shenker, E. Silverstein and J. Simon. This work is supported by the Israel Science Foundation, by the Braun-Roger-Siegl foundation, by EU-HPRN-CT-2000-00122, by GIF, by Minerva, by the Einstein Center and by the Blumenstein foundation.

REFERENCES

1. T. Hertog and G. T. Horowitz, *JHEP* **0504**, 005 (2005) [arXiv:hep-th/0503071].
2. T. Hertog and G. T. Horowitz, *Phys. Rev. Lett.* **94**, 221301 (2005) [arXiv:hep-th/0412169].
3. T. Hertog, *AIP Conf. Proc.* **743**, 305 (2005) [arXiv:hep-th/0409160].
4. T. Hertog and G. T. Horowitz, *JHEP* **0407**, 073 (2004) [arXiv:hep-th/0406134].
5. T. Banks and W. Fischler, arXiv:hep-th/0606260.
6. T. Banks, W. Fischler and L. Mannelli, *Phys. Rev. D* **71**, 123514 (2005) [arXiv:hep-th/0408076].
7. T. Banks and W. Fischler, arXiv:hep-th/0212113.
8. T. Banks and W. Fischler, arXiv:hep-th/0111142.
9. T. Biswas, R. Brandenberger, A. Mazumdar and W. Siegel, arXiv:hep-th/0610274.
10. M. Gasperini and G. Veneziano, arXiv:hep-th/0703055.
11. J. Khoury, B. A. Ovrut, P. J. Steinhardt and N. Turok, *Phys. Rev. D* **64**, 123522 (2001) [arXiv:hep-th/0103239].
12. M. Banados, M. Henneaux, C. Teitelboim and J. Zanelli, *Phys. Rev. D* **48**, 1506 (1993) [arXiv:gr-qc/9302012].
13. M. Banados, C. Teitelboim and J. Zanelli, *Phys. Rev. Lett.* **69**, 1849 (1992) [arXiv:hep-th/9204099].
14. L. Fidkowski, V. Hubeny, M. Kleban and S. Shenker, *JHEP* **0402**, 014 (2004) [arXiv:hep-th/0306170].
15. P. Kraus, H. Ooguri and S. Shenker, *Phys. Rev. D* **67**, 124022 (2003) [arXiv:hep-th/0212277].
16. A. Giveon, D. Kutasov and N. Seiberg, *Adv. Theor. Math. Phys.* **2**, 733 (1998) [arXiv:hep-th/9806194].
17. G. T. Horowitz and A. R. Steif, *Phys. Lett. B* **258**, 91 (1991).
18. N. A. Nekrasov, *Surveys High Energ. Phys.* **17**, 115 (2002) [arXiv:hep-th/0203112].
19. B. Pioline and M. Berkooz, *JCAP* **0311**, 007 (2003) [arXiv:hep-th/0307280].
20. L. Cornalba, M. S. Costa and C. Kounnas, *Astrophys. Space Sci.* **283**, 517 (2003).
21. L. Cornalba and M. S. Costa, *Class. Quant. Grav.* **20**, 3969 (2003) [arXiv:hep-th/0302137].
22. L. Cornalba, M. S. Costa and C. Kounnas, *Nucl. Phys. B* **637**, 378 (2002) [arXiv:hep-th/0204261].
23. L. Cornalba and M. S. Costa, *Phys. Rev. D* **66**, 066001 (2002) [arXiv:hep-th/0203031].
24. H. Liu, G. W. Moore and N. Seiberg, *JHEP* **0210**, 031 (2002) [arXiv:hep-th/0206182].
25. H. Liu, G. W. Moore and N. Seiberg, *JHEP* **0206**, 045 (2002) [arXiv:hep-th/0204168].
26. J. Simon, *JHEP* **0206**, 001 (2002) [arXiv:hep-th/0203201].
27. A. Giveon, E. Rabinovici and A. Sever, *JHEP* **0307**, 055 (2003) [arXiv:hep-th/0305140].

28. A. Giveon, E. Rabinovici and A. Sever, Fortsch. Phys. **51**, 805 (2003) [arXiv:hep-th/0305137].
29. S. Elitzur, A. Giveon and E. Rabinovici, JHEP **0301**, 017 (2003) [arXiv:hep-th/0212242].
30. S. Elitzur, A. Giveon, D. Kutasov and E. Rabinovici, JHEP **0206**, 017 (2002) [arXiv:hep-th/0204189].
31. V. Balasubramanian, S. F. Hassan, E. Keski-Vakkuri and A. Naqvi, Phys. Rev. D **67**, 026003 (2003) [arXiv:hep-th/0202187].
32. R. Biswas, E. Keski-Vakkuri, R. G. Leigh, S. Nowling and E. Sharpe, JHEP **0401**, 064 (2004) [arXiv:hep-th/0304241].
33. V. a. Belinsky, I. m. Khalatnikov and E. m. Lifshitz, Adv. Phys. **31** (1982) 639.
34. V. A. Belinsky, I. M. Khalatnikov and E. M. Lifshitz, Adv. Phys. **19** (1970) 525.
35. R.M. Wald, "General Relativity", University of Chicago Press.
36. C. W. Misner, In **J R Klauder, Magic Without Magic**, San Francisco 1972, 441-473
37. T. Damour, M. Henneaux and H. Nicolai, Class. Quant. Grav. **20**, R145 (2003) [arXiv:hep-th/0212256].
38. B. Berger, "Numerical approaches to space-time singularities", Living reviews in relativity.
39. D. Garfinkle, Phys. Rev. Lett. **93**, 161101 (2004) [arXiv:gr-qc/0312117].
40. S. W. Hawking, Phys. Rev. D **46**, 603 (1992).
41. M. Berkooz, B. Pioline and M. Rozali, JCAP **0408**, 004 (2004) [arXiv:hep-th/0405126].
42. M. Berkooz, B. Craps, D. Kutasov and G. Rajesh, JHEP **0303**, 031 (2003) [arXiv:hep-th/0212215].
43. G. T. Horowitz and J. Polchinski, Phys. Rev. D **66**, 103512 (2002) [arXiv:hep-th/0206228].
44. C. Bachas and M. Porrati, Phys. Lett. B **296**, 77 (1992) [arXiv:hep-th/9209032].
45. C. Bachas, Phys. Lett. B **374**, 37 (1996) [arXiv:hep-th/9511043].
46. M. Berkooz, B. Durin, B. Pioline and D. Reichmann, JCAP **0410**, 002 (2004) [arXiv:hep-th/0407216].
47. M. Berkooz, Z. Komargodski, D. Reichmann and V. Shpitalnik, JHEP **0512**, 018 (2005) [arXiv:hep-th/0507067].
48. J. Scherk and J. H. Schwarz, Phys. Lett. B **82**, 60 (1979).
49. J. McGreevy and E. Silverstein, JHEP **0508**, 090 (2005) [arXiv:hep-th/0506130].
50. E. Silverstein, Phys. Rev. D **73**, 086004 (2006) [arXiv:hep-th/0510044].
51. G. T. Horowitz and J. M. Maldacena, JHEP **0402**, 008 (2004) [arXiv:hep-th/0310281].
52. G. T. Horowitz and E. Silverstein, Phys. Rev. D **73**, 064016 (2006) [arXiv:hep-th/0601032].
53. A. Sen, Int. J. Mod. Phys. A **20**, 5513 (2005) [arXiv:hep-th/0410103].
54. A. Adams, J. Polchinski and E. Silverstein, JHEP **0110**, 029 (2001) [arXiv:hep-th/0108075].
55. G. T. Horowitz, JHEP **0508**, 091 (2005) [arXiv:hep-th/0506166].
56. E. Witten, Adv. Theor. Math. Phys. **2**, 505 (1998) [arXiv:hep-th/9803131].
57. J. L. F. Barbon and E. Rabinovici, JHEP **0203**, 057 (2002) [arXiv:hep-th/0112173].
58. V. Fateev, A. Zamolodchikov and Al. Zamolodchikov, unpublished.
59. V. Kazakov, I. K. Kostov and D. Kutasov, Nucl. Phys. B **622**, 141 (2002) [arXiv:hep-th/0101011].
60. A. Giveon and D. Kutasov, JHEP **0001**, 023 (2000) [arXiv:hep-th/9911039].
61. A. Giveon and D. Kutasov, JHEP **9910**, 034 (1999) [arXiv:hep-th/9909110].
62. S. F. Ross, JHEP **0510**, 112 (2005) [arXiv:hep-th/0509066].
63. A. Adams, X. Liu, J. McGreevy, A. Saltman and E. Silverstein, JHEP **0510**, 033 (2005) [arXiv:hep-th/0502021].
64. J. B. Hartle and S. W. Hawking, Phys. Rev. D **28**, 2960 (1983).
65. A. Strominger and T. Takayanagi, Adv. Theor. Math. Phys. **7**, 369 (2003) [arXiv:hep-th/0303221].
66. S. Fredenhagen and V. Schomerus, JHEP **0312**, 003 (2003) [arXiv:hep-th/0308205].
67. E. Silverstein, arXiv:hep-th/0602230.
68. Y. Nakayama, S. J. Rey and Y. Sugawara, arXiv:hep-th/0606127.
69. O. Aharony and E. Silverstein, Phys. Rev. D **75**, 046003 (2007) [arXiv:hep-th/0612031].

70. S. Hellerman and I. Swanson, arXiv:hep-th/0612116.
71. S. Hellerman and I. Swanson, arXiv:hep-th/0612051.
72. S. Hellerman and I. Swanson, arXiv:hep-th/0611317.
73. J. M. Maldacena, Adv. Theor. Math. Phys. **2**, 231 (1998) [Int. J. Theor. Phys. **38**, 1113 (1999)] [arXiv:hep-th/9711200].
74. N. Iizuka, D. Kabat, G. Lifschytz and D. A. Lowe, Phys. Rev. D **65**, 024012 (2002) [arXiv:hep-th/0108006].
75. D. Kabat, G. Lifschytz and D. A. Lowe, Phys. Rev. D **64**, 124015 (2001) [arXiv:hep-th/0105171].
76. D. Kabat, G. Lifschytz and D. A. Lowe, Int. J. Mod. Phys. A **16**, 856 (2001) [arXiv:hep-th/0007051].
77. D. Kabat and G. Lifschytz, Nucl. Phys. B **571**, 419 (2000) [arXiv:hep-th/9910001].
78. N. Itzhaki, J. M. Maldacena, J. Sonnenschein and S. Yankielowicz, Phys. Rev. D **58**, 046004 (1998) [arXiv:hep-th/9802042].
79. J. M. Maldacena, JHEP **0304**, 021 (2003) [arXiv:hep-th/0106112].
80. L. Fidkowski and S. Shenker, arXiv:hep-th/0406086.
81. G. Festuccia and H. Liu, arXiv:hep-th/0611098.
82. G. Festuccia and H. Liu, JHEP **0604**, 044 (2006) [arXiv:hep-th/0506202].
83. S. D. Mathur, Fortsch. Phys. **53**, 793 (2005) [arXiv:hep-th/0502050].
84. T. Banks, W. Fischler, S. H. Shenker and L. Susskind, Phys. Rev. D **55**, 5112 (1997) [arXiv:hep-th/9610043].
85. R. Dijkgraaf, E. P. Verlinde and H. L. Verlinde, Nucl. Phys. B **500**, 43 (1997) [arXiv:hep-th/9703030].
86. E. J. Martinec, D. Robbins and S. Sethi, JHEP **0608**, 025 (2006) [arXiv:hep-th/0603104].
87. B. Craps, A. Rajaraman and S. Sethi, Phys. Rev. D **73**, 106005 (2006) [arXiv:hep-th/0601062].
88. D. Robbins and S. Sethi, JHEP **0602**, 052 (2006) [arXiv:hep-th/0509204].
89. B. Craps, S. Sethi and E. P. Verlinde, JHEP **0510**, 005 (2005) [arXiv:hep-th/0506180].
90. T. Banks, W. Fischler, I. R. Klebanov and L. Susskind, JHEP **9801**, 008 (1998) [arXiv:hep-th/9711005].
91. T. Banks, W. Fischler, I. R. Klebanov and L. Susskind, Phys. Rev. Lett. **80**, 226 (1998) [arXiv:hep-th/9709091].